



## Effects of Heat Transfer on Combustion Characteristics in a Cylindrical Vortex Combustor

Mohd Fathurrahman Kamarudin<sup>1,2</sup>, Mohd Al-Hafiz Mohd Naw<sup>2,\*</sup>, Azri Hariz Roslan<sup>2</sup>, Muhammad Lutfi Abd Latif<sup>2</sup>, Hazrin Jahidi Jaafar<sup>2</sup>, Mohd Hazwan Mohd Hanid<sup>2,3</sup> Mohd Danish<sup>4</sup>

<sup>1</sup> Politeknik Tuanku Syed Sirajuddin, Pauh Putra, 02600 Arau, Perlis, Malaysia

<sup>2</sup> Faculty of Mechanical Engineering & Technology, Kampus Alam UniMAP, Pauh Putra, 02600 Arau, Perlis, Malaysia

<sup>3</sup> Faculty of Mechanical Engineering, Universiti Teknologi Malaysia, 81310 UTM Skudai, Johor, Malaysia

<sup>4</sup> Department of Mechanical and Materials Engineering, University of Jeddah, Jeddah, 21589, Saudi Arabia

### ARTICLE INFO

### ABSTRACT

#### Article history:

Received 22 August 2024

Received in revised form 20 September 2024

Accepted 23 October 2024

Available online 30 November 2024

#### Keywords:

Heat transfer; Meso-scale combustor;  
Vortex combustions; Equivalence ratio;  
CFD

A vortex flows in micro/meso scale combustors for small-scale power generation play a crucial role in enhancing combustion efficiency and stability. They enhance mixing between fuel and air, promoting better combustion and help stabilize flames by maintaining consistent fuel-air ratios. The temperature are significantly impacts the reactant temperature due to heat conduction wall in Cylindrical Vortex Combustor (CVC). This phenomenon, known as preheating, occurs as the wall transfers heat to the reactants. ANSYS Fluent software is used for conducted a numerical investigation on a CVC. The combustor was characterized by a prescribed mass flow rate of 40 mg/s and an equivalence ratio ( $\phi$ ) ranging from 0.5 to 1.5. Our analysis aimed to understand the combustion behavior within this confined geometry, considering factors such as heat loss and temperature behavior. The numerical findings indicate that elevated equivalence ratios correlate with the highest flame temperature in micro-combustion. Specifically, at an equivalence ratio of  $\phi=0.5$ , the flame temperature remains consistently low compared to the higher value of  $\phi=1.5$ . However, when accounting for wall temperature effects, the maximum flame temperature occurs at an equivalence ratio of  $\phi=1.3$ . The heat dissipation region is quite limited, especially at low equivalence ratio. In summary, heat transfer in cylindrical vortex combustors (CVC) contribute to reliable and efficient power generation, making them essential for portable energy systems.

## 1. Introduction

In the pursuit of resource conservation, environmental friendliness, energy efficiency, and superior engine performance, the design requirements for combustion chambers have become increasingly stringent [1]. In this context, one of these requirements results in low emissions during combustion. Among the various combustion technologies, the vortex combustor has garnered

\* Corresponding author.

E-mail address: [alhafiznawi@unimap.edu.my](mailto:alhafiznawi@unimap.edu.my) (Mohd Al-Hafiz Mohd Naw)

attention for its capacity to reduce pollutants and minimize overall pressure loss in industrial settings [1].

Findings from the previous study [2,3], the utilization of vortex generators [4] and bluff bodies contributes significantly to the overall hydrodynamic flow resistance in the combustion process. The mitigation of Nitrogen Oxides (NOx) emissions can potentially be achieved through the establishment of optimal flow dynamics [5], facilitated by appropriate vortex generation, the composition of bluff bodies, and the adjustment of the initial fuel-air mixture [6,7]. The importance of combustion efficiency and environmental impact requires precise design specifications for combustion devices especially in small scale combustion like meso/micro combustions [8,9]. Ensuring the ideal combination of fuel and oxidant, often air, is crucial for achieving full combustion. According to this viewpoint, the present work conducts computational analyses of a basic combustion device model with preliminary fuel mixing based on the fuel-oxidant flow which to investigate the temperature profile characteristics within the influence of fuel-air mass flow rate through equivalence ratio ( $\phi$ ).

## 2. Methodology

### 2.1 Governing Equations

As followed by previous study [10] the following methods was adopted which are the Cartesian coordinates of the 3D steady-state Favre-averaged governing equations for mass, momentum, species mass fraction, and energy [11]:

$$\frac{\partial \rho \tilde{u}_j}{\partial x_j} = 0 \quad (1)$$

$$\frac{\partial \rho \tilde{u}_i \tilde{u}_j}{\partial x_j} = -\frac{\partial P}{\partial x_i} + \frac{\partial}{\partial x_j} \left[ (\mu + \mu_t) \left( \frac{\partial \tilde{u}_i}{\partial x_j} + \frac{\partial \tilde{u}_j}{\partial x_i} \right) \right] \quad (2)$$

$$\frac{\partial \rho \tilde{u}_i \tilde{Y}_n}{\partial x_j} = \frac{\partial}{\partial x_j} \left[ \left( \rho D_n + \frac{\mu_t}{Sc_t} \right) \left( \frac{\partial \tilde{Y}_n}{\partial x_j} \right) \right] + \dot{\omega}_n \quad (3)$$

$$\frac{\partial \rho \tilde{u}_j \tilde{H}}{\partial x_j} = \frac{\partial}{\partial x_j} \left[ \lambda \frac{\partial \tilde{T}}{\partial x_j} + \frac{\mu_t}{Pr_t} \frac{\partial \tilde{h}}{\partial x_j} + \sum_{n=1}^N \rho D_n h_n \frac{\partial \tilde{Y}_n}{\partial x_j} \right] - \sum_{n=1}^N h_n^f \dot{\omega}_n \quad (4)$$

where  $\rho$  represent the density,  $u_{ij}$  refer to the velocity vector components,  $P$  stand for the pressure,  $\lambda$  stand for the thermal conductivity,  $Pr_t$  indicate the turbulent Prandtl number,  $D_n$  define the mass diffusivity of species ( $n$ ) which is assumed to be constant for each species,  $Y_n$  represent the mass fraction of species ( $n$ ),  $\omega_n$  present the chemical reaction rate,  $\mu$  represent the dynamic viscosity, and  $\mu_t$  represent the turbulent viscosity and the  $\sim$  denotes the Favre averaging [12,13].

### 2.2 Computational Procedures

The current study employed a three-dimensional finite volume solver to discretize the flow domain. This discretization is achieved using a second-order upwind scheme. A variety of triangular grids have been constructed to ensure grid-independence of the solution. The Semi-Implicit Method for Pressure-Linked Equations (SIMPLE) algorithm has been implemented to achieve mass conservation between the velocity components and pressure in the discretized momentum equation. In the present investigation, we have considered the chemical reaction within a volumetric framework. To model the intricate interactions between turbulence and chemistry, we have opted

for the Eddy-Dissipation (ED) algorithm. Moreover, the ED reaction model intentionally omits detailed chemical kinetics and instead relies exclusively on the governing parameters inherent to the reactive flow. Furthermore, the operating conditions were meticulously set at a pressure of 1.01 bars and a temperature of 300 K. A steady-state pressure-based solver was utilized to solve the governing equations using the Computational Fluid Dynamics (CFD) code ANSYS Fluent in all simulations [10]. The schematic representation of the asymmetric vortex combustor is depicted in Figure 1, while the corresponding dimensions are enumerated in Table 1.

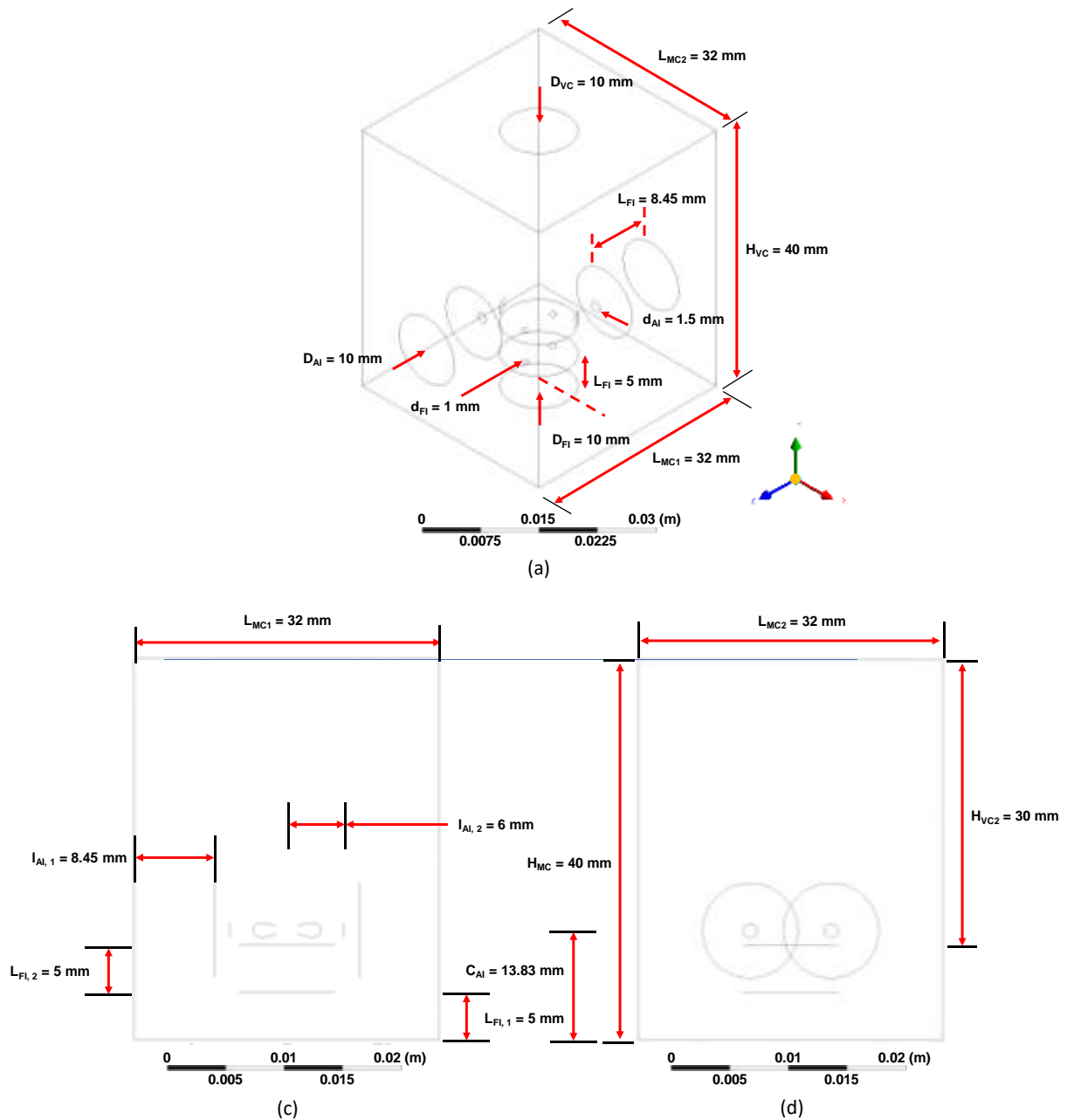


Fig. 1. Design of the vortex combustor; (a) isometric views, (b) side views and (c) front views

The wall of steel material, a common choice for such applications due to its mechanical strength and thermal properties. The thermal boundary condition at the wall is a mixed heat transfer mode with a heat transfer coefficient,  $h$ , of  $20 \text{ W/m}^2 \text{ K}$ . The ambient temperature for the simulation is set at 300 K. This comprehensive setup, combining advanced models and carefully defined boundary

conditions, provides a robust framework for investigating the complex phenomena under study. The results from this study will contribute to our understanding of these systems and inform the design and operation of similar systems in the future. The data extraction process was examined with reference line to varying axis, inside dan outside wall temperature, (A, B and C), as depicted in Figure 2. To streamline this extraction, six distinct lines were established within the vortex combustor chamber. The initial line is situated 30 mm downstream of the air and fuel inlet, with subsequent lines spaced at intervals of 5 mm. The final line is positioned 50 mm upstream of the pressure outlet. These lines, designated as interior, do not influence the computational fluid dynamics (CFD) calculations.

**Table 1**

Dimensions of the cylindrical vortex combustor

Dimensions	Units (mm)
$L_{MC1}$	32
$L_{MC2}$	32
$H_{MC}$	40
$H_{VC}$	30
$L_{FI}$ (length fuel inlet)	5
$L_{AI}$ (length air inlet)	8.45
$d_{AI}$ (air inlet small diameter)	1.5
$d_{FI}$ (fuel inlet small diameter)	1
$D_{FI}$ (fuel inlet diameter)	10
$D_{AF}$ (air inlet diameter)	10
$D_{VC}$ (vortex combustor diameter)	10

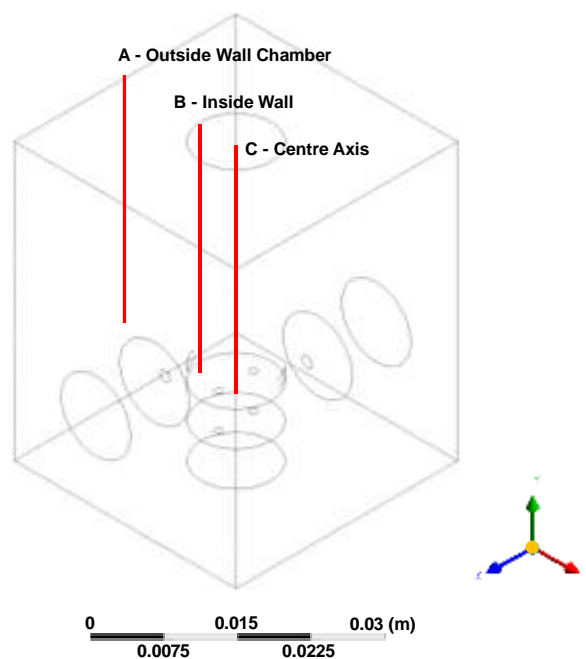


**Fig. 2.** Line reference for data extractions

Close to the finding by Khaleghi *et al.*, [10], the convergence of the solution is deemed to have been achieved when the residuals of each governing equation in successive iterations. Under these conditions, the flow field variables attained stable local values irrespective of the number of iterations. Additionally, the parameter of temperature was monitored separately for convergence. This convergence criterion was applied to reacting flow cases [10]. A laminar flow with a counter-

flow arrangement was employed for this examination, with the inlet air and fuel temperatures both established at 300 K. The computational realm of the vortex combustor encompassed both the solid and fluid domains. These computations were executed on a computer equipped with a Core i9 processor and 16 GB of RAM.

Moreover, as followed by the previous researcher, Khaleghi *et al.*, [13], the present study employs the K-epsilon (Eq. (2)) RNG Viscos model, specifically configured for a swirl dominated flow option, to simulate asymmetric vortex mixture. The radiation effects are accounted for using the Discrete Ordinate (DO) model, which provides a robust solution for radiative heat transfer. The chemical reactions within the flow are modeled using the Volumetric Species Transport Reaction model, coupled with an Eddy Dissipation model for turbulence-chemistry interaction. This combination allows for a comprehensive representation of the complex interplay between chemical reactions and turbulence in the flow. The boundary conditions (Figure 3(a)) are meticulously defined to reflect the physical scenario under investigation. The air inlet is characterized by variable velocities, a temperature of 300 K, and a composition of 23% O<sub>2</sub> and 77% N<sub>2</sub>. Similarly, the fuel inlet conditions include variable velocities, a temperature of 300 K, and a high concentration of CH<sub>4</sub> at 97% [10]. The mass flow rate for the air inlet were set to 40 mg/s and for fuel inlet (methane gas) were set in range of 2.50E-6 to 3.76E-6 at equivalence ratio ( $\phi$ ) of 0.5 until 1.5. It can be seen from Figures 6(a) and 6(b), and Figures 7(a) and 7(b).

In accordance with Figure 3(b), the process of meshing is applied to the entire enclosure. The objective is to confine the mesh sizing within a specific control volume. This approach significantly reduces the computational time required for running the simulation. A grid sensitivity analysis was conducted to assess the influence of grid dimensions on the outcomes, as depicted in Figure 4. Five (5) sets of triangular meshes were constructed, each with a different number of nodes. The number of elements in each set are as follows: M1 = 1,365,755 nodes, M2 = 642,781 nodes, M3 = 337,718 nodes, M4 = 222,738 nodes and M5 = 153,999 nodes. The study revealed that the chamber exhibited nearly equal findings when subjected to 337,718 nodes.

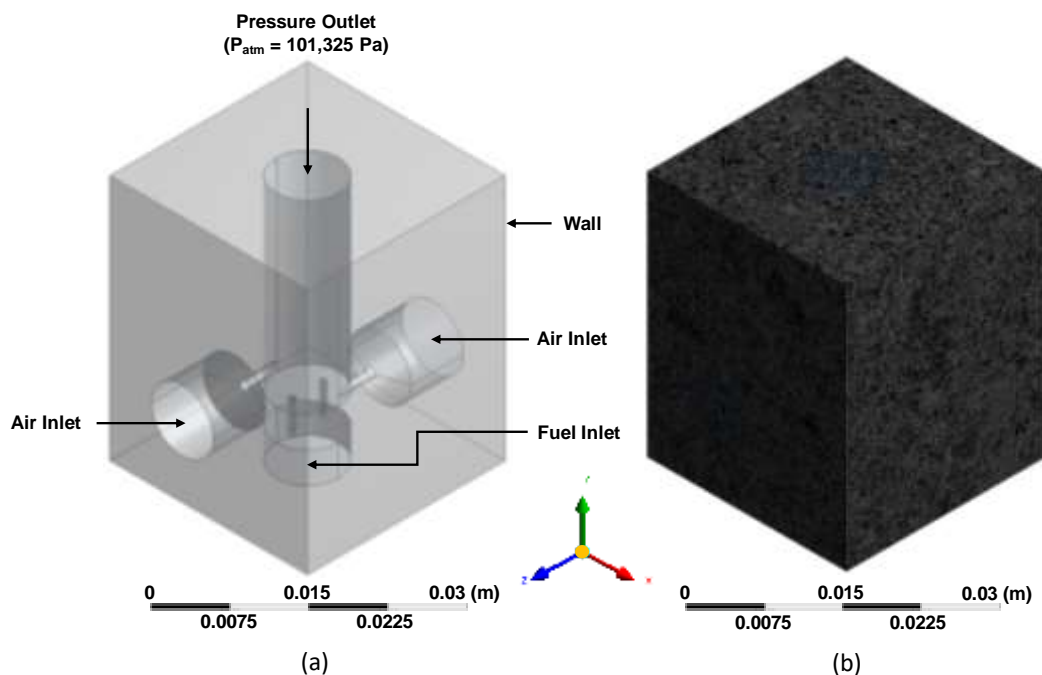


Fig. 3. Cylindrical Vortex Combustor; (a) Meshing and (b) boundary conditions

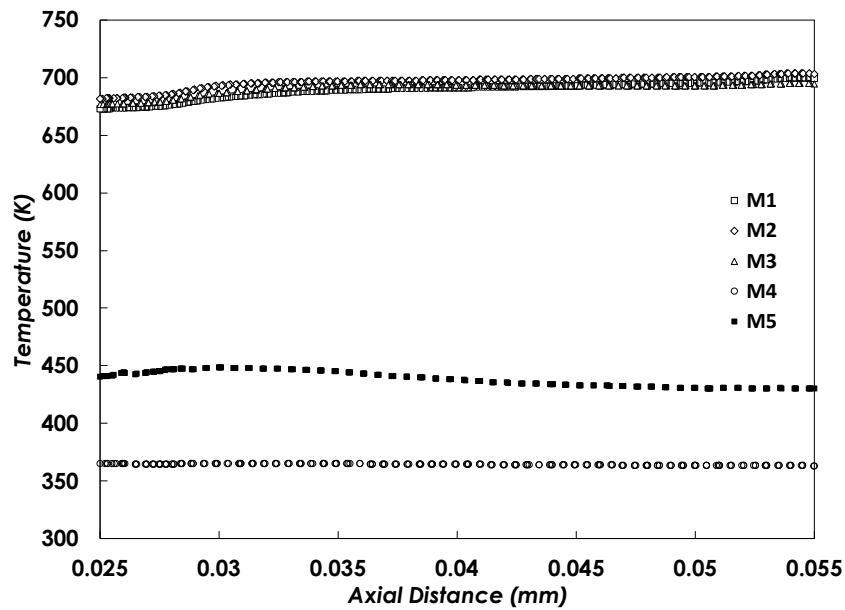


Fig. 4. Computational grid independence study

### 3. Results

#### 3.1 Temperature Distributions

Figure 5 illustrates a direct correlation between the local temperature within the central axis of the combustor and the escalation of the equivalency ratio. As the equivalency ratio rises, there is an observable augmentation in the concentration of hot-flow volume within the core section of the combustor. The investigation's outcomes indicate an elevated temperature within the proximal central area near the exit plane of the combustor, attributed to the existence of a flame tip. This flame tip manifests in the vicinity of the exit plane under conditions characterized by a high mass flow rate of air. This result was in line with previous study by Khaleghi *et al.*, [10], who found that enhancement of the equivalency ratio,  $\phi$  in the vortex combustor's centre, the hot flow would require greater quantities.

The diagram depicted in Figure 5 delineates the schematic represent the temperature of centre axis along with axial distances in a cylindrical vortex combustor. According to the data presented in Figure 6(a) and 6(b), the temperature of the inner wall exceeds that of the outer wall owing to its closer proximity to the combustion flame. Nevertheless, the temperature disparity between the outer wall and the inner temperature remains relatively inconsequential. Mainly, towards at the lower section of the chamber, the internal and external temperatures exhibit approximate parity. However, progressing longitudinally along the chamber, once the equivalence ratio rises the temperature at one-third of the combustor was increase and the temperature is readily observable at the exit of the vortex combustor chamber. This phenomenon can be attributed to the rise in mass flow rate, particularly the fuel mass flow rate contribution. Moreover, at the area of one-third of the vortex combustor, the temperature in the area appears to rise due to the hill's form, which likely facilitates the storage of a substantial quantity of fuel-air mixes for combustion.

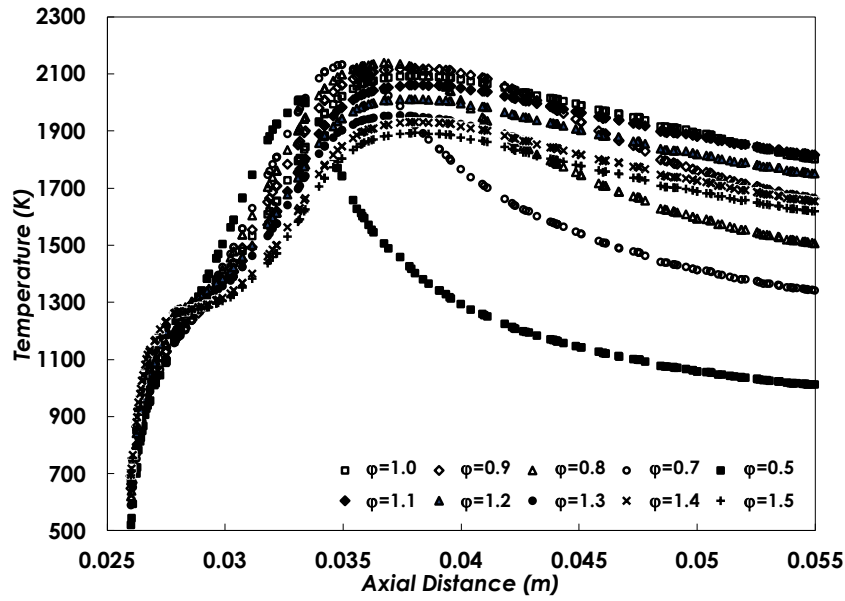


Fig. 5. Temperature distributions along the central axis of cylindrical vortex combustion for different equivalence ratio ( $\phi$ ) = 0.5-0.9

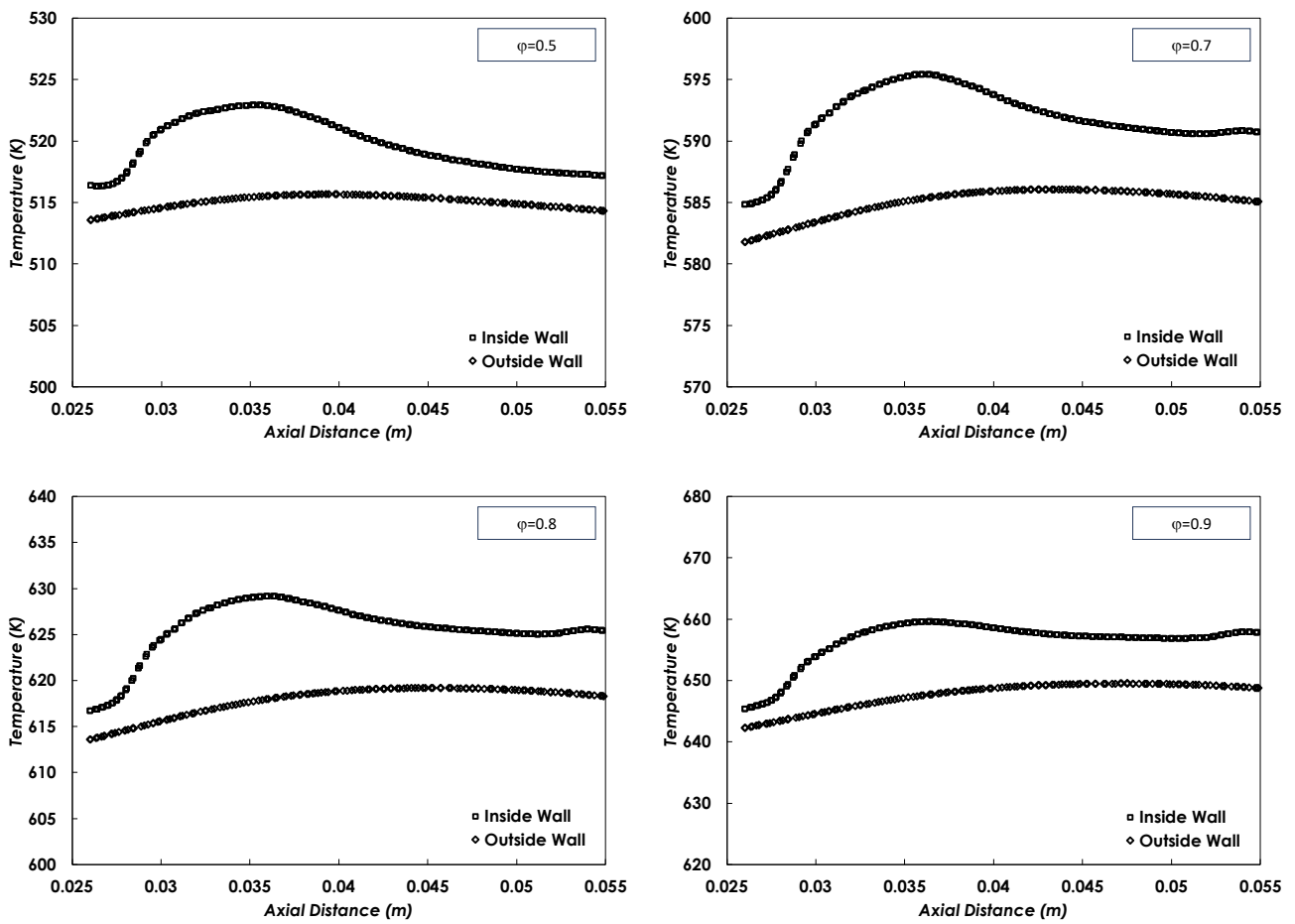
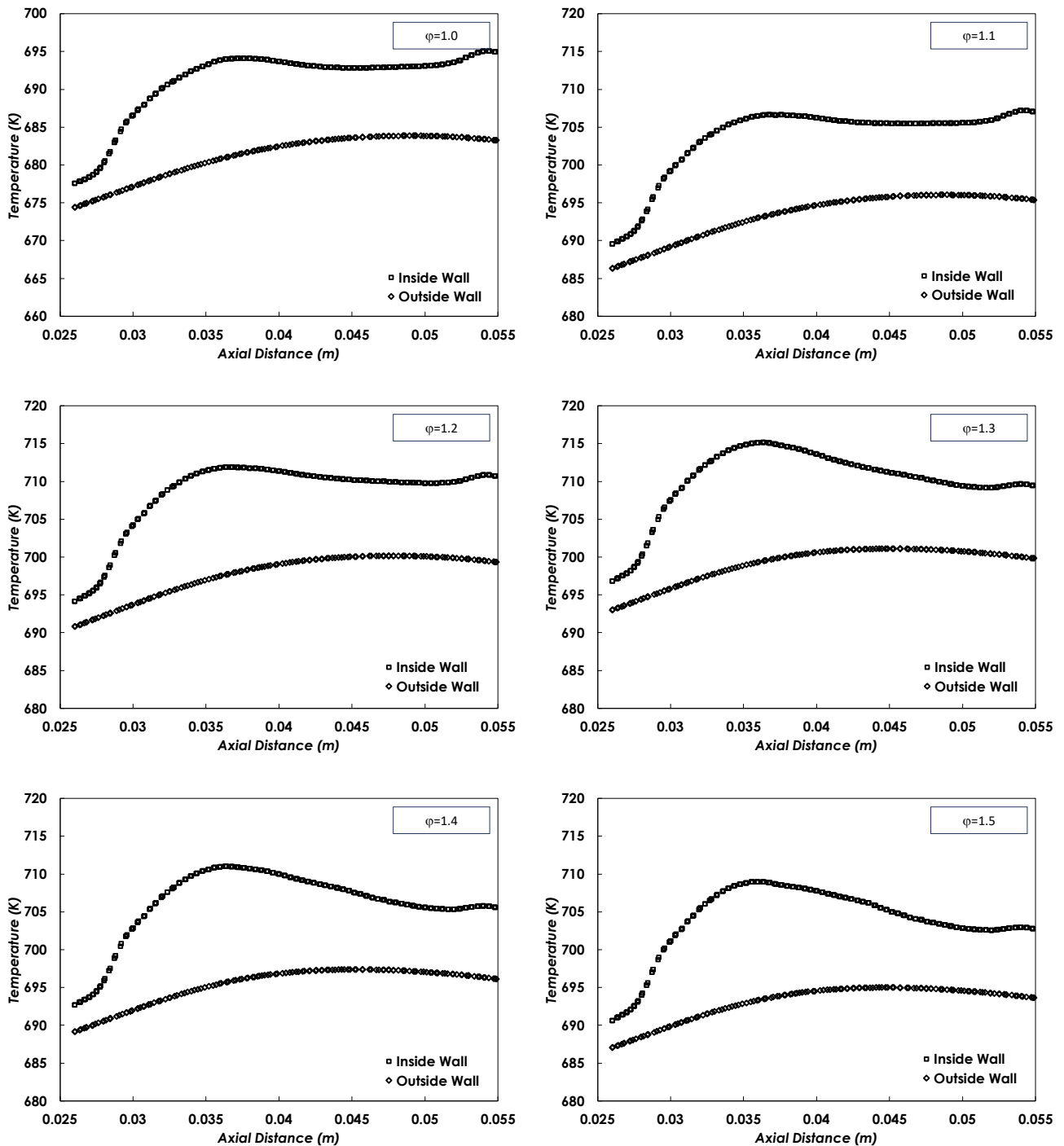


Fig. 6(a). Wall temperature of cylindrical vortex combustor (CVC) at different equivalence ratio ( $\phi$ ) = 0.5-0.9 (continued)



**Fig. 6(b).** Wall temperature of cylindrical vortex combustor (CVC) at different equivalence ratio ( $\phi$ ) = 1.0-0.5

### 3.2 Flame Structure

A clear 2D temperature profiles of vortex flames on what is happening in the vortex combustion chamber can be referred to Figure 7(a) and 7(b). As already mentioned by previous researcher, Khaleghi *et al.*, [10], the need for establishing a theory regarding the aerodynamic stability mechanism of these flames dictates their significance. Due to the findings of the current temperature profiles corresponds to the case with the equivalence ratio ( $\phi$ ) of 0.5-1.5 were acceptable compared to the previous study [1]. The temperature distribution is visualized across distinct planes, revealing



the inherent asymmetry within the reactive flow field. As shown in Figure 7(a), where the temperature distribution is relatively low especially at  $\phi=0.5$ . Based on the contour flame, the combustion process exhibits low temperature. This issue may arise due to insufficient heat transfer to the air-fuel combination, resulting in failure to satisfy the necessary conditions for combustion. Additionally, low centrifugal forces may cause the air-fuel mixture to be deflected towards the wall. Therefore, the ideal circumstances for the combustion process cannot be achieved. Nevertheless, when the equivalence ratio was increased by focusing to  $\phi=0.9$ , it was discovered that the temperature downstream of the asymmetry was comparatively high and yields increased vortices generation.

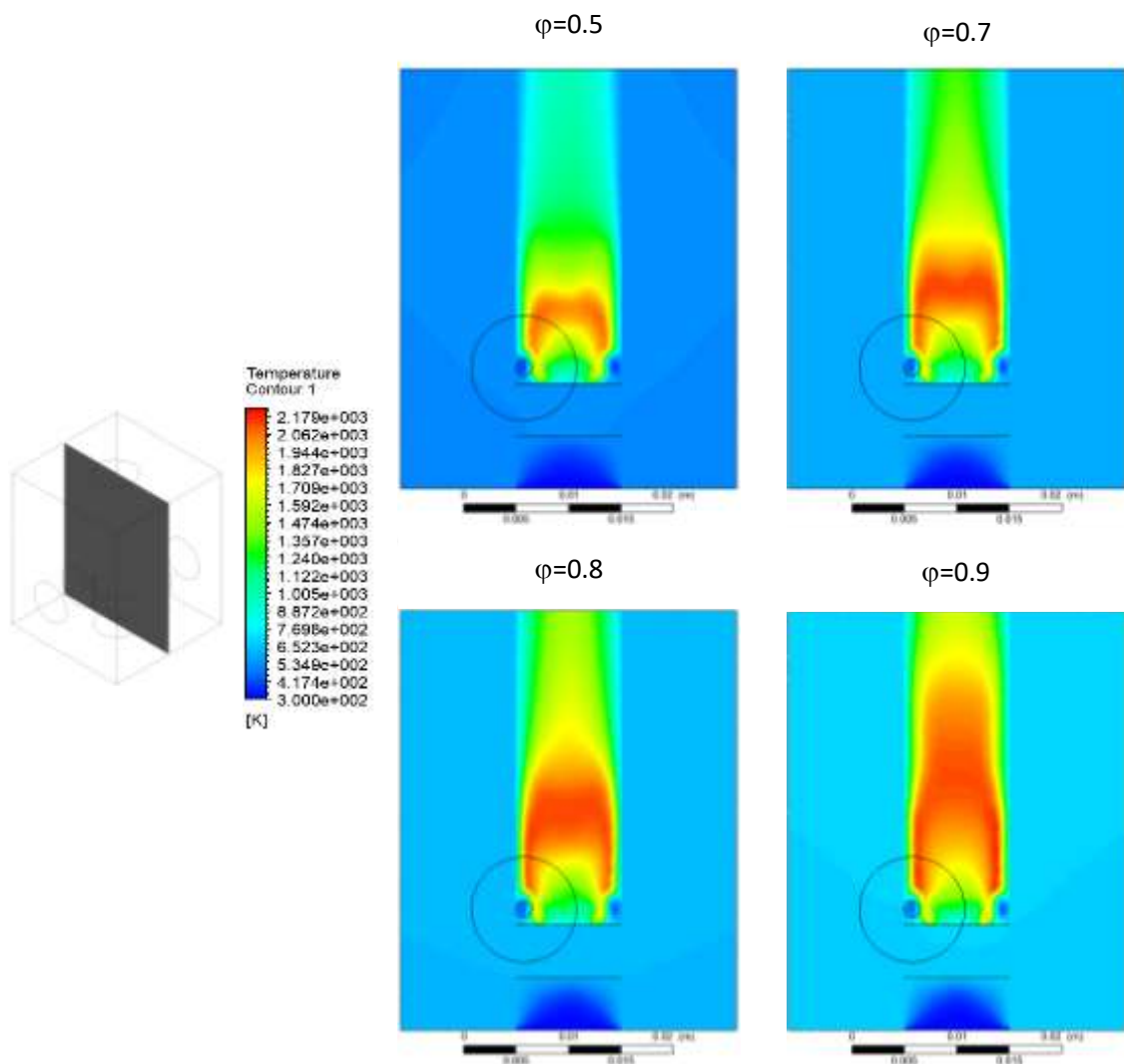


**Fig. 7(a).** Contour of temperature profiles at different equivalence ratio ( $\phi$ ) = 0.5-0.9 (continued)

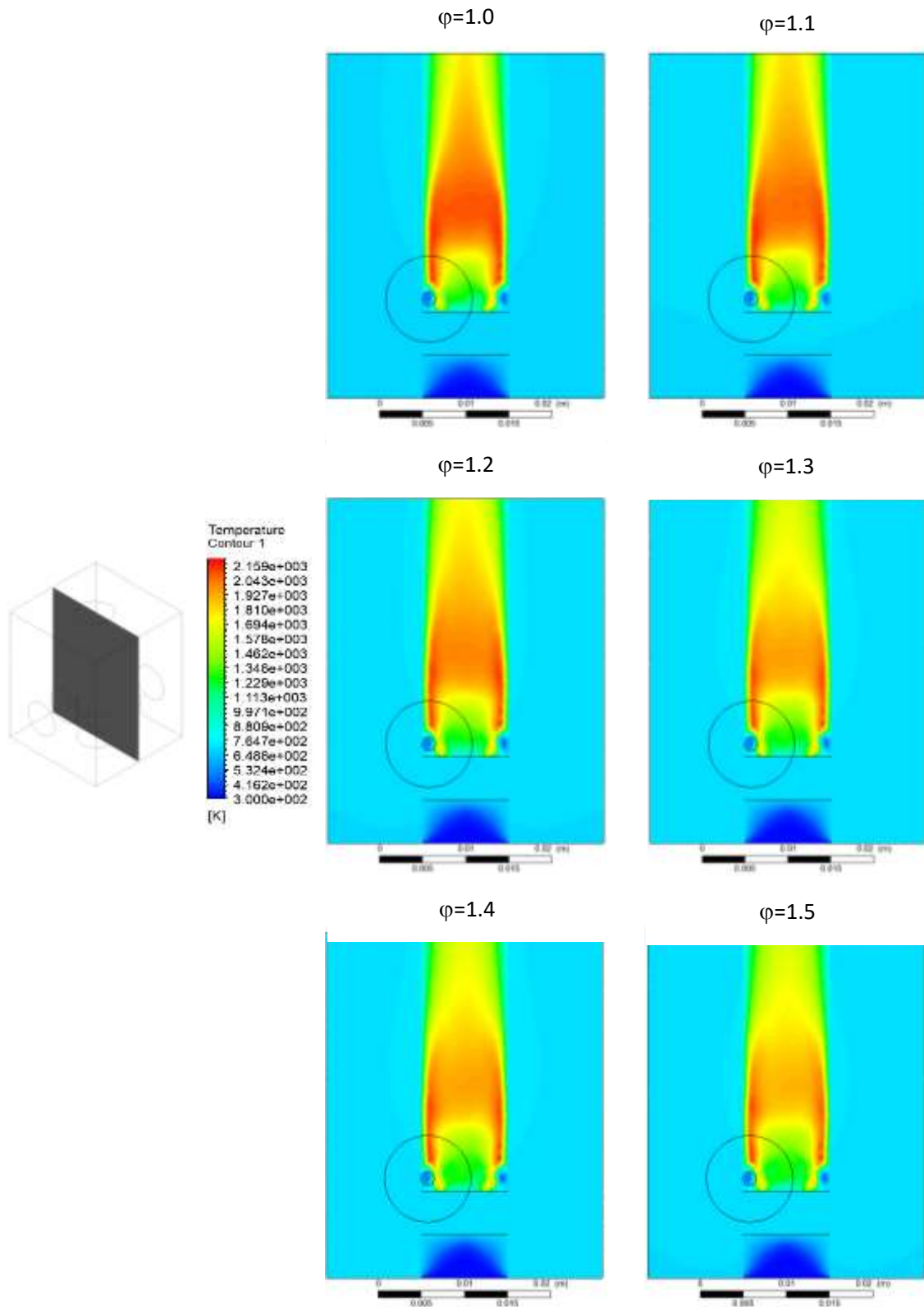


Fig. 7(b). Contour of temperature profiles at different equivalence ratio ( $\phi$ ) = 1.0-1.5

By referring to equivalence ratio ( $\phi$ ) of 1.2-1.5, the flame exhibits a nearly symmetrical configuration, wherein at two-thirds from downstream region the area was elevated temperature. As the swirling of the flow increases (effected by rises equivalence ratio), the flow turbulence also increases, and the shape of the flame becomes asymmetrical. Compared to Rahman and Yusup [14] and Pannala *et al.*, [15] same characteristics of the outcomes pertaining to CH<sub>4</sub>-Air combustion reveal that the resultant combustion gases exhibit proximity to both the CVC centreline and the adjacent combustor wall. Moreover, swirl combustors are the biggest enhancements to the GT combustion system because they can stabilise the flame across a broad range of equivalency ratios [16-18]. This can be seen at equivalence ration ( $\phi$ ), 0.7, 0.8, 1.0 and 1.1. Due to a greater central recirculation zone and a higher swirling flow velocity, the hot flow occupies bigger volumes in the central region of the combustor as the equivalence ratio ( $\phi$ ) increases under stoichiometric conditions. This finding is consistent with Khaleghi *et al.*, [13]. Moreover, according to geometry, this zone represents the area where the fuel-air undergo mixtures. The next phenomenon can be defined to the amplification of turbulence size and turbulence fluctuations, which ultimately result in the ignition of an asymmetrically shaped flame.

#### 4. Conclusions

This study examines the properties of the combustion process occurring inside cylindrical vortex combustor. Numerical simulations investigating the impact of the vortex generator have demonstrated the temperature behaviour through selected equivalence ratio ( $\phi$ ) which affects vigorous swirling motion of airflow. The observed outcome indicates that air-fuel mixtures, influenced by centrifugal forces, exhibit directed motion along the burner wall. Additionally, within the context of asymmetrical vortex combustion systems, flow recirculation manifests. Consequently, the combustion process is adversely affected, leading to reduced combustion efficiency. Moreover, premixed combustion in a cylindrical vortex combustion chamber in this investigation showed that an excess of combustible fuel increased the rate of combustion.

#### Acknowledgement

The research has been carried out under the Fundamental Research Grant Scheme (FRGS) (FRGS-EC/1/2024/TK08/UNIMAP/02/31) provided by the Ministry of Higher Education.

#### References

- [1] Zheng, Baisen, Yueliang Zhang, and Jin Xie. "Investigation of performance in a cylindrical trapped vortex combustor with swirler." *Heat and Mass Transfer* 59, no. 6 (2023): 1121-1137. <https://doi.org/10.1007/s00231-022-03319-7>
- [2] Vignat, Guillaume, Daniel Durox, Kevin Prieur, and Sébastien Candel. "An experimental study into the effect of injector pressure loss on self-sustained combustion instabilities in a swirled spray burner." *Proceedings of the Combustion Institute* 37, no. 4 (2019): 5205-5213. <https://doi.org/10.1016/j.proci.2018.06.125>
- [3] Chen, Zhichao, Qingxiang Wang, Bingnan Wang, Lingyan Zeng, Miaomiao Che, Xin Zhang, and Zhengqi Li. "Anthracite combustion characteristics and NO<sub>x</sub> formation of a 300 MWe down-fired boiler with swirl burners at different loads after the implementation of a new combustion system." *Applied energy* 189 (2017): 133-141. <https://doi.org/10.1016/j.apenergy.2016.12.063>
- [4] Sies, Mohsin Mohd, and Mazlan Abdul Wahid. "Numerical investigation of the asymmetrical vortex combustor running on biogas." *Journal of Advanced Research in Fluid Mechanics and Thermal Sciences* 74, no. 1 (2020): 1-18. <http://dx.doi.org/10.37934/arfmts.74.1.118>
- [5] Su, Xianqiang, Qingyan Fang, Lun Ma, Bin Yao, Yuan Li, Xinpeng Zhao, Rui Mao, and Chungen Yin. "Improving combustion and lowering NO<sub>x</sub> emissions of an industrial coal swirl burner by optimizing its nozzle structure." *Applied Thermal Engineering* 218 (2023): 119340. <https://doi.org/10.1016/j.applthermaleng.2022.119340>
- [6] Li, Zhengqi, Song Li, Qunyi Zhu, Xiqian Zhang, Guipeng Li, Yong Liu, Zhichao Chen, and Jiangquan Wu. "Effects of particle concentration variation in the primary air duct on combustion characteristics and NO<sub>x</sub> emissions in a 0.5-

- MW test facility with pulverized coal swirl burners." *Applied thermal engineering* 73, no. 1 (2014): 859-868. <http://dx.doi.org/10.1016/j.applthermaleng.2014.08.041>
- [7] Khanafer, K., and S. M. Aithal. "Fluid-dynamic and NOx computation in swirl burners." *International Journal of Heat and Mass Transfer* 54, no. 23-24 (2011): 5030-5038. <https://doi.org/10.1016/j.ijheatmasstransfer.2011.07.017>
- [8] Hosseini, Seyed Ehsan, Evan Owens, John Krohn, and James Lylek. "Experimental investigation into the effects of thermal recuperation on the combustion characteristics of a non-premixed meso-scale vortex combustor." *Energies* 11, no. 12 (2018): 3390. <https://doi.org/10.3390/en11123390>
- [9] Saputro, Herman, Laila Fitriana, Aris Purwanto, Fudhail A. Munir, and Wei-Cheng Wang. "A Development of Meso-Scale Vortex Combustion for a Micro Power Generator Based on a Thermoelectric Generator." *Fluids* 7, no. 12 (2022): 386. <https://doi.org/10.3390/fluids7120386>
- [10] Khaleghi, Mostafa, Seyed Ehsan Hosseini, and Mazlan A. Wahid. "Vortex combustion and heat transfer in meso-scale with thermal recuperation." *International Communications in Heat and Mass Transfer* 66 (2015): 250-258. <https://doi.org/10.1016/j.icheatmasstransfer.2015.06.005>
- [11] Obieglo, A., J. Gass, and D. Poulikakos. "Comparative study of modeling a hydrogen nonpremixed turbulent flame." *Combustion and flame* 122, no. 1-2 (2000): 176-194. [http://dx.doi.org/10.1016/S0010-2180\(00\)00114-0](http://dx.doi.org/10.1016/S0010-2180(00)00114-0)
- [12] Saqr, K. M., M. M. Sies, and M. A. Wahid. "Numerical investigation of the turbulence-combustion interaction in nonpremixed CH<sub>4</sub>/air flames." *International Journal of Applied Mathematics and Mechanics* 5, no. 8 (2009): 69-79. <http://doi.org/10.2514/1.B35217>
- [13] Khaleghi, Mostafa, Seyed Ehsan Hosseini, and Mazlan Abdul Wahid. "Investigations of asymmetric non-premixed meso-scale vortex combustion." *Applied Thermal Engineering* 81 (2015): 140-153. <https://doi.org/10.1016/j.applthermaleng.2015.02.022>
- [14] Rahman, Mohammad Nurizat, and Suzana Yusup. "Large Eddy Simulation of Hydrogen/Natural Gas/Air Premixed Swirling Flames and CIVB Flashback Risks." *CFD Letters* 15, no. 12 (2023): 154-165. <https://doi.org/10.37934/cfdl.15.12.154165>
- [15] Pannala, Sreekanth, Vladimir Shtern, Lei Chen, and David West. "Novel Annular Jet Vortex Reactor for High-Temperature Thermochemical Conversion of Hydrocarbons to Acetylene." *ACS Engineering Au* 2, no. 5 (2022): 406-420. <https://doi.org/10.1021/acsengineeringau.2c00009>
- [16] Rahman, Mohammad Nurizat, Mohd Fairus Mohd Yasin, and Mohd Shiraz Aris. "Reacting flow characteristics and multifuel capabilities of a multi-nozzle dry low NOx combustor: A numerical analysis." *CFD Letters* 13, no. 11 (2021): 21-34. <https://doi.org/10.37934/cfdl.13.11.2134>
- [17] Rahman, Mohammad Nurizat, Norshakina Shahril, and Suzana Yusup. "Hydrogen-Enriched Natural Gas Swirling Flame Characteristics: A Numerical Analysis." *CFD Letters* 14, no. 7 (2022): 100-112. <https://doi.org/10.37934/cfdl.14.7.100112>
- [18] Rahman, Mohammad Nurizat, and Suzana Yusup. "Large Eddy Simulation of Hydrogen/Natural Gas/Air Premixed Swirling Flames and CIVB Flashback Risks." *CFD Letters* 15, no. 12 (2023): 154-165. <https://doi.org/10.37934/cfdl.15.12.154165>